Hindawi
Advances in Civil Engineering
Volume 2020, Article ID 8867375, 9 pages
https://doi.org/10.1155/2020/8867375

Research Article

Permeability Properties of Crushed Stone Aggregates in Bedding Course of Urban Permeable Roads: An Experimental Study

Rongrong Mao and Haiyan Yang

Jiangsu Shipping College, Nantong, Jiangsu 226010, China

Correspondence should be addressed to Rongrong Mao; maorongrong8@126.com

Received 21 August 2020; Revised 10 October 2020; Accepted 19 October 2020; Published 31 October 2020

Academic Editor: Hualei Zhang

Copyright © 2020 Rongrong Mao and Haiyan Yang. This is an open access article distributed under the Creative Commons Attribution License, which permits unrestricted use, distribution, and reproduction in any medium, provided the original work is properly cited.

Crushed stone is the most common material for use in the aggregate of bedding course. The aggregate for the bedding course of permeable roads needs to not only meet the requirements of basic mechanical properties but also ensure permeability and structural stability. This work analyzed permeability under extreme rainfall conditions and the particle mass loss during permeation and then investigated the stability of crushed stone aggregate and examined the optimal gradation and compaction levels of the crushed stone aggregate in engineering applications. It shows that (1) the permeation process included two phases, and the change of permeation velocity mainly occurred in the first phase. The permeation velocity of samples with different gradations at different compaction levels showed a stepwise change in its order of magnitude. (2) The change in permeability coincided with the change in flowrate, most probably because the sudden change of the flow altered the permeability of the sample. Factors such as gradation, compaction, and the randomness of particles arrangement in the crushed stone during sample charging all affected the permeability of the sample. (3) During the permeation process, the mass loss decreased with rising gradation. The gradation and compaction had strong influence on particle mass loss. Therefore, ensuring the structural stability of permeable road necessitates careful selection of the gradation and compaction for the crushed stone aggregate. It is recommended to use the crushed stone sample with a gradation of $n = 0.7$ and a compaction level of no greater than 20 mm for the aggregate of the bedding course.

1. Introduction

Presently, most roads in Chinese cities use impervious pavement. The drawbacks of impervious pavement include the following. (1) It disrupts the natural circulation of water and prevents precipitation from replenishing groundwater because it lacks the permeability of soil and vegetation. (2) It obstructs the heat and water exchange between the air and the ground and worsens the "heat island" effect in urban areas because it releases massive amount of absorbed solar heat. (3) It tends to cause accumulation of water and eventually leads to urban flooding [1–3]. To address these problems, Germany took the lead in 1960 by constructing porous asphalt pavements. Since the 1980s, impervious pavement is increasingly replaced around the globe by permeable asphalt, permeable tile, cobble stone-like pavement, etc., to improve the permeability so that rainwater can rapidly infiltrate into soil to reduce soil erosion, conserve water sources, and improve regional ecological environments [3–5].

Extensive works have been carried out on the pavement and the bedding course of permeable roads. Watanabe S. [1] studied the runoff control of permeable pavement at an area in Yokohama, Japan. Schluter and Jeffries [2] studied how the porosity of the filling in the permeable pavement could affect the water flow at the exit of parking lot and help reduce peak runoff. Benedetto [3] used permeable pavement to promote infiltration and mitigate the accumulation of water caused by rainfall at an airport. From a field study on the long-term permeability of the permeable concrete pavement and brick pavement, Borgwardt and Chen [4] found that the permeability of these pavements decreased by several orders of magnitude after several years of use, and the size of the filler particles determined the permeability. Beeldens et al.

[5] gave an overview of various permeable roads in Belgium from the monitoring data of newly completed projects of permeable pavement in Belgium and the test data of permeable pavement after nearly 15 years of use. The measurement data showed that these roads had good performance and long-lasting permeability. They compared and analyzed the permeability data, investigated how the use of permeable roads would impact urban sustainable drainage management, and discussed promoting the application of permeable roads through legislation. Wang et al. [6] proposed the use of permeable pavement to allow rainwater to infiltrate soil, conserve groundwater, and regulate urban ecological environment. Wang et al. [7, 8] examined the relationship between urban permeable pavement and urban ecology. Wu et al. [9] used a homemade simulated rainfall system to experimentally study typical bedding materials such as impervious tiles, cement floors, permeable tiles, and grass. Ding et al. [10] studied the optimal mix ratio and production technology of materials for permeable roads through extensive experiments on the raw materials and manufacturing processes. Zhang [11] used in-situ permeameter, single-ring permeameter, double-ring permeameter, and other instruments to test the permeation of permeable recyclable pellets under constant and variable hydraulic head to compare the applicability of different test methods of permeability coefficient. Zhang et al. [12] found that the permeability of concrete permeable bricks decreased with their service life. In the first two years, the permeable bricks generally showed good permeable effect, but their permeable property weakened significantly after two years. Hou et al. [13, 14] studied permeable brick pavements with different bedding course structures and found that the use of permeable brick pavement could significantly reduce surface runoff. The surface runoff coefficient was always lower when permeable brick was used instead of impervious brick, and the infiltration depended on the bedding course structure of the permeable brick. Meng et al. [15] examined representative permeable roads in Shanghai to survey the actual permeability, summarize the current application of permeable roads, and analyze the key factors of permeability. Related works [12–16] show that the bedding course of permeable road directly affects the permeability, and it is thus essential to study the permeability of the bedding course.

Crushed stone is the most common material for use in the aggregate of bedding course. Because of extreme rainfall [17, 18] and continuous rain erosion, the migration and loss of particulate matter in the aggregate of bedding course will take place and undermine the structural stability of the bedding course.

In this work, we considered the use of crushed stone as the aggregate in the bedding course of urban permeable roads, examined the permeability of crushed stone as well as the loss of particulate matter under rain erosion, and investigated the choice of gradation and compaction of bedding course aggregate. Specifically, we used a continuous grading mixture to simulate the bedding course and tested the infiltration speed, the permeability of the mixture, and the material migration in the permeation experiments. We then analyzed the impact of gradation and compaction on the permeability and mass loss of particulate matter in the bedding course.

2. Materials and Methods

2.1. Sample Preparation. The bedding course of roads is commonly laid using crushed stone of different particle sizes because the gaps between larger particles can be filled by smaller particles. However, the filling particles should be smaller than the gap distance so as to avoid the interference between large and small particles. Therefore, particles of different sizes should be mixed based on a certain ratio [19]. In the current test, crushed stone was sieved into five different sizes, i.e., 0–5 mm, 5–10 mm, 10–15 mm, 15–20 mm, and 20–25 mm, and Talbot continuous grading [20] was adopted:

$$p(d) = \left(\frac{d_i}{d_M}\right)^n \times 100\%, \tag{1}$$

where $p(d)$ is the percentage of particles whose size is no larger than d_i, and d_M is the maximum particle size. The mass of particles of each size is

$$M_{d_i}^{d_{i+1}} = \left[\left(\frac{d_{i+1}}{d_M}\right)^n - \left(\frac{d_i}{d_M}\right)^n\right] \times M_T, \tag{2}$$

where M_T is the total mass of the sample, and d_i and d_{i+1} are adjacent particle sizes.

Wang et al. showed that when the Talbot power index n is 0.1 and 0.2, the content of fine particles is relatively high, which is likely to cause instability [21, 22]. Therefore, the current test considered n values of 0.4, 0.5, 0.6, and 0.7. The mass of each sample is 2 kg in the test, and the mass of particles of different sizes is given in Table 1. Four different compaction levels (10 mm, 20 mm, 30 mm, and 40 mm) were evaluated to analyze the impact of compaction level on particle loss and permeability over time.

2.2. Permeability Test System. Figure 1 illustrates the homemade permeability test system [23] for broken rock with variable mass, which was adopted in this work to test the permeability of crushed stone aggregate. The system consists of an axial load and displacement control module, a permeation module, and a data acquisition and analysis module. A particle recovery module is added to measure mass loss.

The axial load and displacement control module includes a material testing machine, a single acting hydraulic cylinder, a variable displacement piston pump, etc. The single-action hydraulic cylinder has the maximum traverse of 50 mm, the variable displacement piston pump has the rated pressure of 31.5 MPa, and the permissions error of ±4%.

The permeation module includes a permeameter, pipelines, a fixed displacement piston pump, a double-acting hydraulic cylinder, etc. The quantitative displacement piston pump can provide a maximum pressure about 8 MPa, and its work pressure is 7 MPa, maximum displacement is about

Table 1: The mass qualities of different diameters broken rock with different Talbot power exponents.

Mass (g)		n			
		0.4	0.5	0.6	0.7
Rock particle sizes	0–5 mm	1050.6	894.4	761.5	648.3
	5–10 mm	335.7	370.5	392.7	404.8
	10–15 mm	244.1	284.3	317.9	345.6
	15–20 mm	198.8	239.7	277.3	312.0
	20–25 mm	170.8	211.1	250.6	289.2

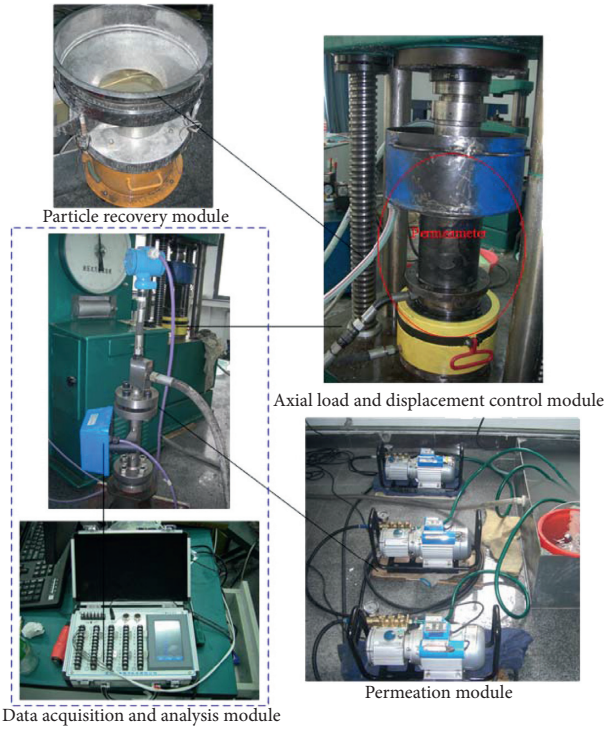

Figure 1: The home-made permeability test system for broken rock with variable mass.

600 L per hour. The double-action hydraulic cylinder with an inner diameter of 220 mm has a piston with a diameter of 160 mm, and its maximum traverse and volume are 500 mm and 20 L, respectively.

The data acquisition and analysis module includes displacement sensors, flow sensors, pressure sensors, data collectors, PC, etc. The particle recovery module includes vibrating sieves, filter cloths, an oven, an electronic scale, etc. The filter screen is the 300 meshes fine gauze, and the corresponding collected grains size could reach 48 microns. The pressure transducer has the measure traverse and measure accuracy of 16 MPa and 2 kPa, respectively.

2.3. Test Procedure. Figure 2 shows the test process. The sample's initial height was measured after the sample was charged. Because manual charging gave highly variable porosity, after being packed into the permeameter, samples were firstly subjected to 0.02 MPa at 1 mm/min for preliminary compression without crushing the particles. The

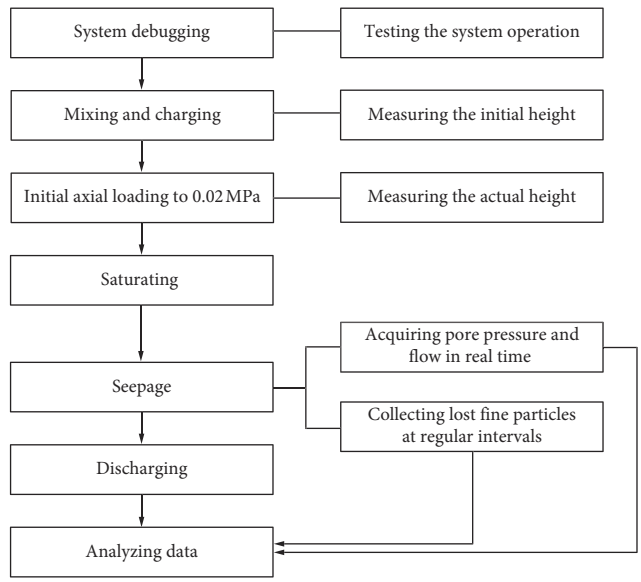

Figure 2: The test process.

sample's actual height was then measured at this point based on the displacement of the testing machine. Water was then injected to saturate the sample and start the permeation test. The pressure and flow data were recorded in real-time during the test. The lost particles were collected at defined intervals because they could not be measured in real-time. The mass loss of particles was relatively high at the start of the test and the interval for particle collection was initially set to 2 min. The collection interval could then be gradually increased as the mass loss decreased over time.

3. Results and Analysis

From the permeability test of the crushed stone aggregate, data such as water pressure, flowrate, and particle mass loss during permeation in the sample were measured, and the change of physical quantities such as permeation velocity, permeability, and particle loss were calculated and rationalized.

3.1. Variation of Permeation Velocity. During the test, the flowrate Q was measured in real-time, from which the permeation velocity v could be calculated as follows:

$$v = \frac{Q}{\pi a^2}, \tag{3}$$

where a is the inner radius of the permeameter ($a = 50$ mm).

The permeation velocity was calculated from the real-time flow in the test. Figure 3 shows that the permeation process includes two phases corresponding to fast mass loss and slow permeation, respectively, and the change in permeation velocity mainly occurred in the slow permeation phase. During fast mass loss, the permeation velocity increased because of rising porosity that resulted from the migration and loss of small particles. Figure 3 shows that the duration of the mass loss stage varied for different samples

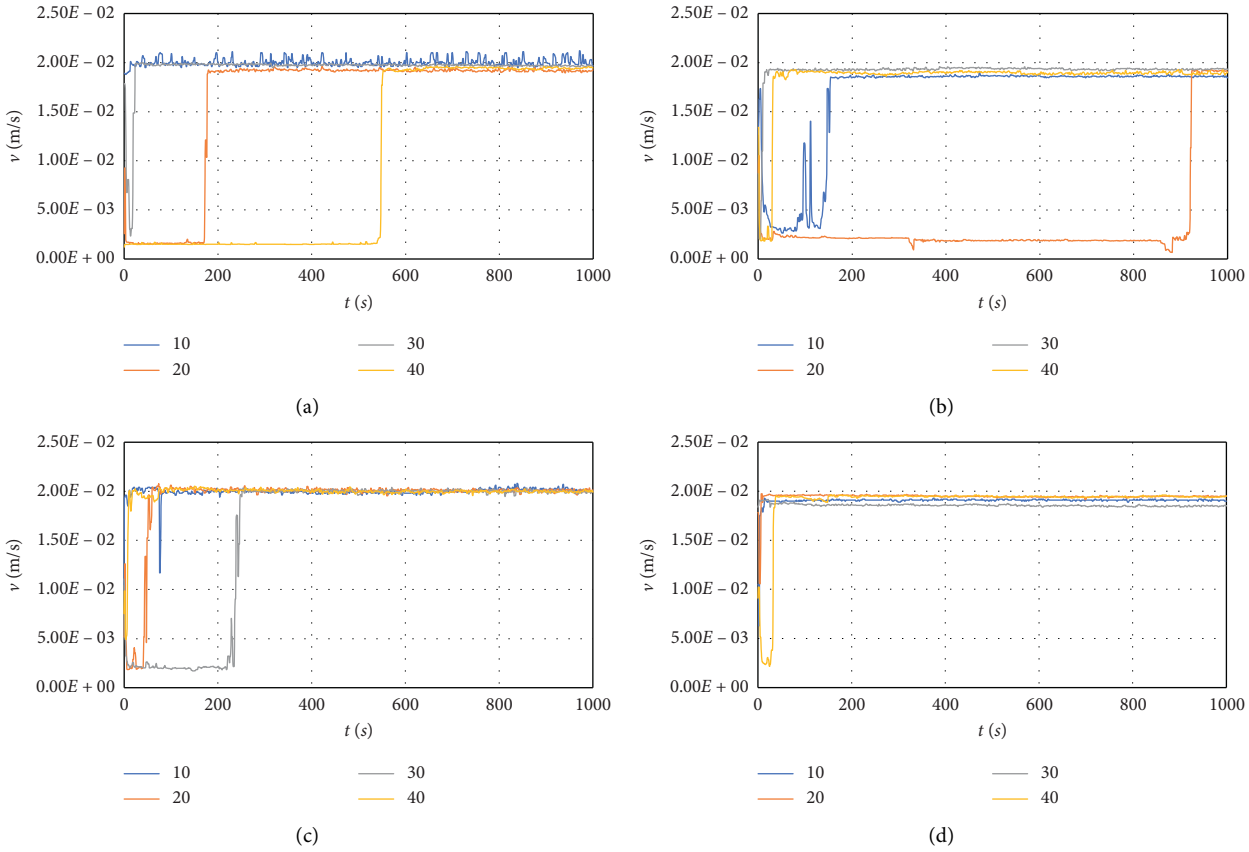

Figure 3: The permeation velocity of the mass loss stage varied for different samples. (a) $n = 0.4$. (b) $n = 0.5$. (c) $n = 0.6$. (d) $n = 0.7$.

because their contents of small particles that could migrate were different. The content of small particles was the smallest for the $n = 0.7$ sample, whose mass loss phase lasted for only as short as 50 s. In contrast, the $n = 0.4$ and $n = 0.5$ samples had a relatively longer mass loss phase because they had a higher content of small particles. Particularly, for the $n = 0.5$ sample with initial compaction of 20 mm, the mass loss phase lasted for nearly 930 s.

Table 2 also shows a stepwise increase in the order of magnitude of the permeation velocity for samples with different gradations at different levels of compaction. For the $n = 0.4$ and $n = 0.5$ samples, the permeation velocity always increased from the order of 10^{-3} m/s to the order of 10^{-2} m/s regardless of compaction level. For the $n = 0.6$ samples, the permeation velocity remained at the 10^{-2} m/s level throughout the test when the initial compaction was 10 mm but showed a lower initial permeation velocity at the 10^{-3} m/s level with higher initial compactions. For the $n = 0.7$ samples, the initial permeation velocity was at the 10^{-2} m/s level when the initial compactions were 10–30 mm but decreased to the 10^{-3} m/s level when the initial compaction increased to 40 mm. Therefore, the initial compaction level had a significant impact on the permeation velocity and affected the permeation velocity at the beginning of the test.

3.2. Variation of Permeability. Lu et al. [24, 25] used a home-made permeameter to analyze the flow characteristics of

Table 2: The change of magnitudes of permeation velocity in the whole test.

	10 mm	20 mm	30 mm	40 mm
0.4	10^{-3}~10^{-2}	10^{-3}~10^{-2}	10^{-3}~10^{-2}	10^{-3}~10^{-2}
0.5	10^{-3}~10^{-2}	10^{-3}~10^{-2}	10^{-3}~10^{-2}	10^{-3}~10^{-2}
0.6	10^{-2}~10^{-2}	10^{-3}~10^{-2}	10^{-3}~10^{-2}	10^{-3}~10^{-2}
0.7	10^{-2}~10^{-2}	10^{-2}~10^{-2}	10^{-2}~10^{-2}	10^{-3}~10^{-2}

permeable pavement mixtures under different hydraulic gradients. The results show that Darcy's law is not applicable to analyzing directional water transport in permeable pavement materials. With rising hydraulic gradient, the Reynolds number of permeable pavement materials increases, and the water flow in permeable pavement materials transitions from Darcy flow to non-Darcy flow.

The Forchheimer equation was used to describe the non-Darcy flow of the permeation process for the aggregate in this paper:

$$-\nabla p = \frac{\mu}{k} v + \rho \beta v^2, \tag{4}$$

where ∇p is the pressure gradient, μ is the dynamic viscosity of the fluid, k is the permeability, ρ is the fluid density, and β is the non-Darcy factor.

The permeability k and non-Darcy factor β in Equation (4) are the two key parameters that describe the permeability characteristics of crushed stone, and they can be calculated

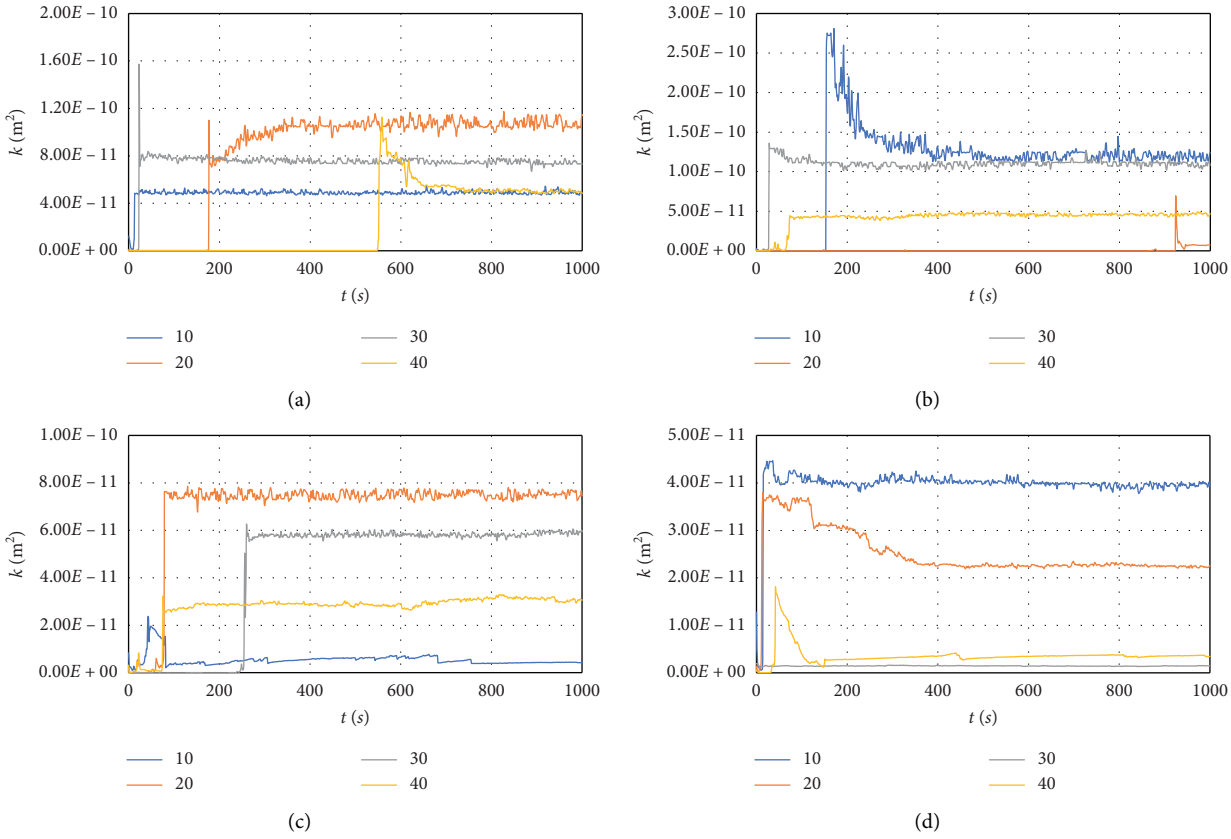

FIGURE 4: The permeability of samples with different gradation under different compaction levels varied with time. (a) $n = 0.4$. (b) $n = 0.5$. (c) $n = 0.6$. (d) $n = 0.7$.

from the time series of the permeation velocity and the pressure gradient collected in the test [26]:

$$k = \frac{\mu\left[\left(\sum_{i=1}^{n} v_i^3\right)^2 - \sum_{i=1}^{n} v_i^2 \sum_{i=1}^{n} v_i^4\right]}{\sum_{i=1}^{n} \Delta p_i v_i^2 \sum_{i=1}^{n} v_i^3 - \sum_{i=1}^{n} \Delta p_i v_i \sum_{i=1}^{n} v_i^4},$$
$$\beta = \frac{\sum_{i=1}^{n} \Delta p_i v_i \sum_{i=1}^{n} v_i^3 - \sum_{i=1}^{n} \Delta p_i v_i^2 \sum_{i=1}^{n} v_i^2}{\rho\left[\left(\sum_{i=1}^{n} v_i^3\right)^2 - \sum_{i=1}^{n} v_i^2 \sum_{i=1}^{n} v_i^4\right]}. \quad (5)$$

Figure 4 shows how the permeability of samples with different gradation under different compaction levels varied with time. The permeability of all samples was at the order of 10^{-11}–10^{-10} m^2 during the entire permeation process. The permeability of all samples showed a sharp increase in the rapid mass loss phase, and the increase was concomitant with the sudden change of flowrate. It can be speculated that the sudden change of the flow led to the change of the samples' permeability. In the later part of the permeation test, the permeability only demonstrated minor vacillation and remained basically unchanged. In addition, gradation and compaction levels also affected the permeability of the samples. For example, as seen in Figure 4, the $n = 0.5$ sample had the highest permeability of 2.7×10^{-10} m^2, while the $n = 0.7$ sample only had a permeability no greater than 4.4×10^{-11} m^2. The influence of compaction on permeability seemed to be somewhat irregular, possibly due to the randomness of particle arrangement when the samples were charged into the device.

The permeability of the aggregate needs to be considered in selecting aggregates for the bedding course of the permeable road. Ideally, aggregates with relatively high permeability should be chosen.

Figure 5 shows the non-Darcy factors for different samples varied with time. The logarithmic form was used in the figure because the non-Darcy factors varied across several orders of magnitude. Contrary to permeability, the non-Darcy factors gradually decreased as time elapsed [27].

It is worth noting that the change in the permeability of the crushed stone aggregate during the permeation process was related to the particle loss during the test.

3.3. Particle Mass Loss. During the permeation process, small particles of crushed stone were carried by the water flow and left the permeameter [28–31]. The lost particles were collected at given time intervals at Δt_i ($i = 1, 2, 3, \ldots$), as shown in Figure 6, and their mass after drying was weighed and recorded as m_i ($i = 1, 2, 3, \ldots$). In this way, the total mass loss $\sum m_i$ during the permeation process could be calculated. It can be seen from Figure 6 that the size of the lost particles ranged mostly in 0–2 mm, and the amount of collected particles gradually decreased as time elapsed.

Figure 7 shows the mass loss of crushed stone aggregates with different gradations. It could be found that as the

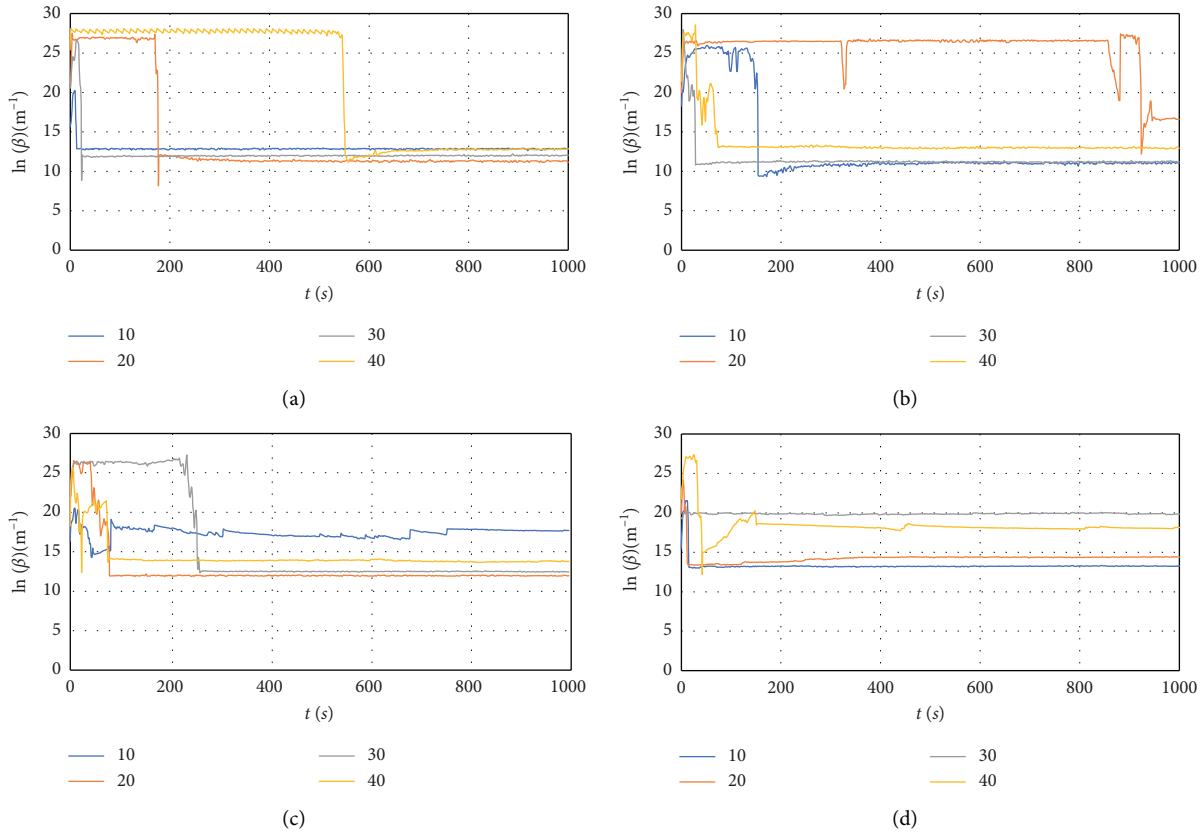

Figure 5: The non-Darcy factor of samples with different gradation under different compaction levels varied with time. (a) $n = 0.4$. (b) $n = 0.5$. (c) $n = 0.6$. (d) $n = 0.7$.

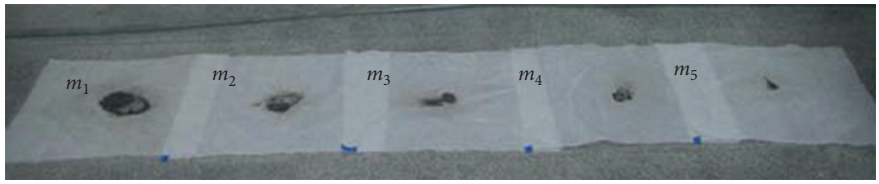

Figure 6: The lost particles collected at given time intervals.

gradation increased the content of fine particles decreased. Although some secondary small particles were produced during the permeation process from water-rock interaction, the mass loss still mainly came from the original small particles. Therefore, the mass loss decreased with rising gradation. The $n = 0.4$ sample had the highest mass loss of about 280 g, while the $n = 0.7$ sample had a maximum mass loss of 48 g, which was only 17% that of the $n = 0.4$ sample.

For samples with the same gradation, the mass loss increased with intensifying compaction. For example, the mass loss of the $n = 0.6$ sample under 40 mm compaction was 452% of its mass loss under 10 mm compaction. In contrast, the mass loss of the $n = 0.5$ sample under 40 mm compaction was 175% of its mass loss under 10 mm compaction. The difference in these increments was related to factors such as gradation and the particle arrangement during sample charging. It could be seen that gradation and compaction have significant impact on the mass loss. In selecting the aggregate of the bedding course for permeable roads, it is crucial to determine the gradation and the corresponding compaction to ensure structural stability.

Figure 7 also shows that the rate of mass loss differed between samples. For example, for samples with the same compaction level of 10 mm, the mass loss rate decreased with rising gradation. The maximum mass loss rate of the $n = 0.4$ and $n = 0.7$ samples reached 8.3 g/s and 0.05 g/s, respectively. The former was 166 times the latter. The mass loss rate of samples with the same gradation but different compaction also varied significantly. For example, the maximum mass loss rate of the $n = 0.5$ sample with 30 mm and 20 mm compaction reached 5.86 g/s and 0.054 g/s, respectively, which were two orders of magnitude apart.

4. Discussion

The permeability, mass loss, and mass loss rate of all samples were classified based on the relevant specifications of permeable roads, with the standard being 2.0×10^{-11} m^2, 100 g,

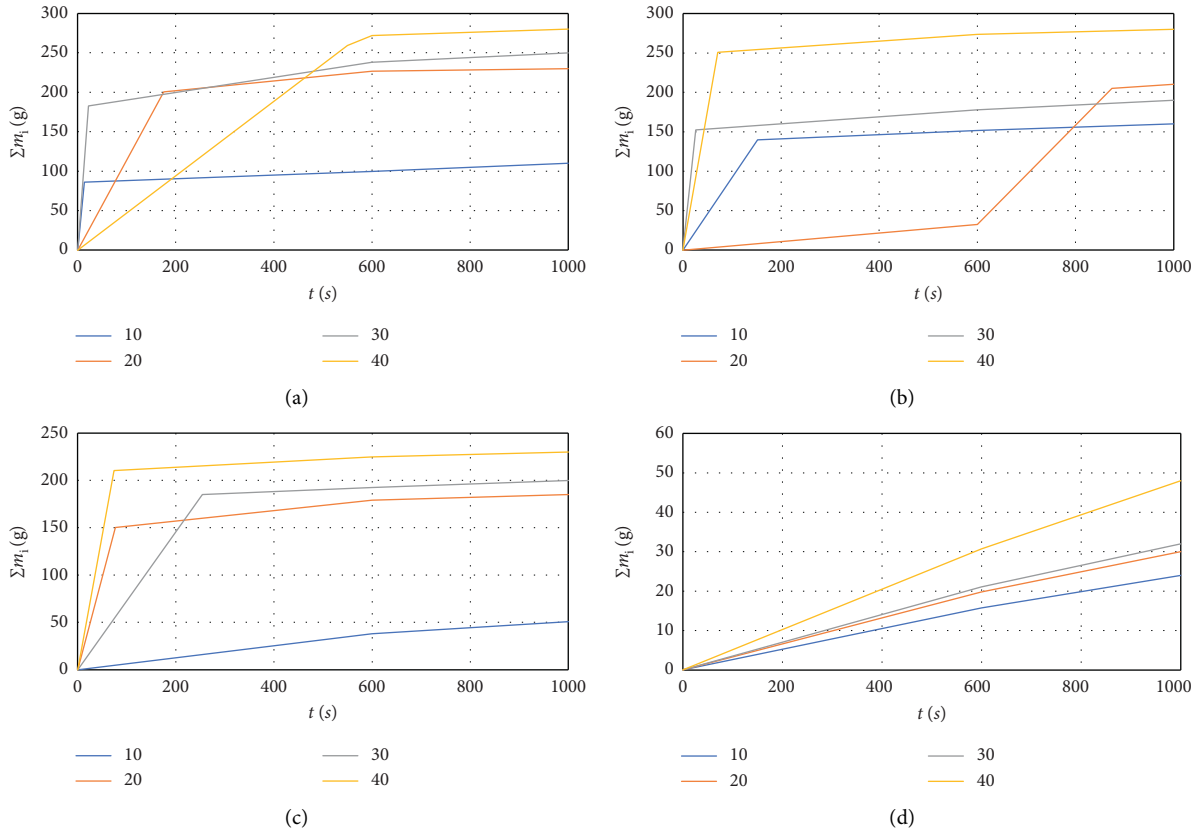

Figure 7: The mass loss of crushed stone aggregates with different gradation. (a) $n = 0.4$. (b) $n = 0.5$. (c) $n = 0.6$. (d) $n = 0.7$.

Table 3: The optimal gradation and compaction levels.

Gradation and initial compression		Permeability	Mass loss	The mass loss rate
0.4	10	R	R	N
	20	R	N	N
	30	R	N	N
	40	R	N	R
0.5	10	R	N	N
	20	U	N	R
	30	R	N	N
	40	R	N	N
0.6	10	N	R	R
	20	R	N	N
	30	R	N	N
	40	R	N	N
0.7	10	R	R	R
	20	R	R	R
	30	N	U	R
	40	N	U	R

and 0.5 g/s, respectively. Accordingly, the tested samples and compactions were categorized into three sets: recommended (R), not recommended (N), and uncertain (U). The optimal gradation and compaction levels were then derived statistically.

It can be found from Table 3 that the permeability of most samples satisfied the requirements as an aggregate for permeable road, but samples with smaller gradation had a higher mass loss during permeation, which may affect the structural stability of the bedding course. For samples with a mass loss less than 5%, structural instability could also occur if the mass loss rate was too high. Thus, the overall recommendation was to use crushed stone with a gradation of $n = 0.7$ and adopt a compaction level of no more than 20 mm in choosing crushed stone as the aggregate for the bedding course of permeable roads. It should be noted that adhesives

were not used in this study. The use of adhesives will change the permeability and particle loss of the bedding course.

5. Conclusions

The aggregate for the bedding course of permeable roads needs to not only meet the requirements of basic mechanical properties such as compressive strength and shear strength but also ensure permeability and structural stability. This work analyzed permeability under extreme rainfall conditions and the particle mass loss during permeation, and then investigated the stability of crushed stone aggregate and examined the optimal gradation and compaction of the crushed stone aggregate in engineering applications. The main conclusions are as follows:

(1) The permeation process included two phases, the first being rapid mass loss and the second being slow permeation. The change of permeation velocity mainly occurred in the first phase. The duration of the rapid mass loss phase varied for samples with different gradations because of their differing amount of small particles that could migrate. The permeation velocity of samples with different gradations at different compaction levels showed a stepwise change in its order of magnitude.

(2) Throughout the permeation process, the permeability of samples with various gradations was all at the order of 10^{-11}–10^{-10} m^2. The change in permeability coincided with the change in flowrate, most probably because of the sudden change of the flow altered the permeability of the sample. Factors such as gradation, compaction, and the randomness of particles arrangement in the crushed stone during sample charging all affected the permeability of the sample.

(3) During the permeation process, the mass loss decreased with rising gradation. The mass loss of the samples with the same gradation generally increased with intensifying compaction. It could be seen that gradation and compaction had strong influence on particle mass loss. Therefore, ensuring the structural stability of permeable road necessitates careful selection of the gradation and compaction for the crushed stone aggregate.

(4) The permeability of most samples could satisfy the requirements as the aggregate, but structural stability of the bedding course of the permeable road may be at stake if the sample had a high mass loss or mass loss rate during permeation. It is recommended to use the crushed stone sample with a gradation of $n = 0.7$ and a compaction level of no greater than 20 mm for the aggregate of the bedding course.

Data Availability

The data used to support the findings of this study are available from the author upon request.

Conflicts of Interest

The authors declare that they have no conflicts of interest.

Acknowledgments

The authors gratefully acknowledge the authors of the references.

References

[1] S. Watanabe, "Study on storm water control by permeable pavement and infiltration pipes," *Water Science and Technology*, vol. 32, no. 1, pp. 25–32, 1995.

[2] W. Schlüter and C. Jefferies, "Modelling the outflow from a porous pavement," *Urban Water*, vol. 4, no. 3, pp. 245–253, 2002.

[3] A. Benedetto, "A decision support system for the safety of airport runways: the case of heavy rainstorms," *Transportation Research Part A: Policy and Practice*, vol. 36, no. 8, pp. 665–682, 2002.

[4] S. Borgwardt and Y. Chen, "Study on long term permeability of permeable concrete pavement brick pavement," *Building Block and Block Building*, vol. 15, no. 2, pp. 37–41, 2008.

[5] A. Beeldens, L. Vijverman, and Y. Cui, "Experience of using permeable pavement with paving brick in Belgium for 15 years—promoting application through legislation," *Building Block and Block Building*, vol. 23, no. 1, pp. 32–38, 2016.

[6] H. Wang, W. Che, and J. Hu, "On storm water infiltration in urban area," *Water and Wastewater Engineering*, vol. 27, no. 2, pp. 4-5, 2001.

[7] B. Wang and C. Li, "Penetrative pavement and urban ecological and physical environment," *Industrial Construction*, vol. 32, no. 12, pp. 29–31, 2002.

[8] B. Wang, "Application of penetrative pavement and its prospects," *Architecture Technology*, vol. 33, no. 9, pp. 659-660, 2002.

[9] S. Wu, Z. Wang, J. Zhang, J. Xie, and Y. Wang, "Experimental study on relationship among runoff coefficients of different underlying surfaces, rainfall intensity and duration," *Journal of China Agricultural University*, vol. 11, no. 5, pp. 55–59, 2006.

[10] Y. Ding, Y. Huang, Z. Ma, Z. Zhong, W. Liu, and B. Cao, "Research of optimum mix proportion of permeable concrete pacing blocks in rainwater harvesting in urban area," *Beijing Water Resources*, vol. 10, no. 1, pp. 12-13, 2003.

[11] N. Zhang, "Comparison and study on test methods for water permeability coefficients of permeable pavement," *Technology of Highway and Transport*, vol. 32, no. 1, pp. 6–9, 2016.

[12] W. Zhang, Y. Ding, and S. Zhang, "Study on water permeability durability of concrete permeable brick," *New Building Materials*, vol. 13, no. 6, pp. 22–24, 2006.

[13] L. Hou, S. Feng, Y. Ding, and S. Zhang, "Runoff-rainfall relationship for multilayer infiltration systems under artificial rainfalls," *Transactions of the Chinese Society of Agricultural Engineering*, vol. 22, no. 9, pp. 100–105, 2006.

[14] L. Hou, S. Feng, Z. Han, Y. Ding, and S. Zhang, "Experimental study on impacts of infiltration treated with porous pavement," *Journal of China Agricultural University*, vol. 11, no. 4, pp. 83–88, 2006.

[15] Y. Meng, T. Li, S. Wang, and Z. Fu, "Field survey and application analysis of infiltration performance of permeable pavements in Shanghai city," *China Water and Wastewater*, vol. 25, no. 6, pp. 29–33, 2009.

[16] L. Huo, *Preparation, Properties of Pervius Concrete Pavement Material*, Southeast University, Nanjing, China, 2004.
[17] L. Xu, Q. Li, Y. Wang, J. Huang, and Y. Xu, "Analysis of the changes in debris flow hazard in the context of climate change," *Climate Change Research*, vol. 16, no. 4, pp. 415–423, 2020.
[18] J.-C. Chen, W.-S. Huang, and Y.-F. Tsai, "Variability in the characteristics of extreme rainfall events triggering debris flows: a case study in the Chenyulan watershed, Taiwan," *Natural Hazards*, vol. 102, no. 3, pp. 887–908, 2020.
[19] ASTM International, *ASTM C39/C39M-15a, Standard test method for compressive strength of cylindrical concrete specimens*, ASTM International, West Conshohocken, PA, USA, 2015.
[20] A. N. Talbot and F. E. Richart, "The strength of concrete and its relation to the cement, aggregate and water," *Bulletin, University of Illinois Engineering Experiment Station*, vol. 11, no. 7, pp. 1–118, 1923.
[21] L. Wang and H. Kong, "Variation characteristics of mass-loss rate in dynamic seepage system of the broken rocks," *Geofluids*, vol. 2018, Article ID 7137601, 17 pages, 2018.
[22] L. Wang, H. Kong, C. Qiu, and B. Xu, "Time-varying characteristics on migration and loss of fine particles in fractured mudstone under water flow scour," *Arabian Journal of Geosciences*, vol. 12, no. 5, p. 159, 2019.
[23] H. Kong and L. Wang, "The mass loss behavior of fractured rock in seepage process: the development and application of a new seepage experimental system," *Advances in Civil Engineering*, vol. 2018, p. 12, Article ID 7891914, 2018.
[24] G. Lu, Z. Wang, P. Liu, D. Wang, and M. Oeser, "Investigation of the hydraulic properties of pervious pavement mixtures: characterization of Darcy and non-Darcy flow based on pore microstructures," *Journal of Transportation Engineering, Part B: Pavements*, vol. 146, no. 2, Article ID 04020012, 2020.
[25] G. Lu, L. Renken, T. Li, D. Wang, H. Li, and M. Oeser, "Experimental study on the polyurethane-bound pervious mixtures in the application of permeable pavements," *Construction and Building Materials*, vol. 202, pp. 838–850, 2019.
[26] D. Ma, X. Cai, Z. Zhou, and X. Li, "Experimental investigation on hydraulic properties of granular sandstone and mudstone mixtures," *Geofluids*, vol. 2018, Article ID 9216578, 13 pages, 2018.
[27] L. Wang, H. Kong, Y. Yin, B. Xu, and D. Zhang, "Strain-based non-Darcy permeability properties in crushed rock accompanying mass loss," *Arabian Journal of Geosciences*, vol. 13, no. 11, p. 406, 2020.
[28] H. Kong and L. Wang, "The behavior of mass migration and loss in fractured rock during seepage," *Bulletin of Engineering Geology and the Environment*, vol. 79, no. 2, pp. 739–754, 2020.
[29] L. Wang, Z. Chen, and H. Kong, "An experimental investigation for seepage-induced instability of confined broken mudstones with consideration of mass loss," *Geofluids*, vol. 2017, Article ID 3057910, 12 pages, 2017.
[30] L. Wang, H. Kong, and M. Karakus, "Hazard assessment of groundwater inrush in crushed rock mass: an experimental investigation of mass-loss-induced change of fluid flow behavior," *Engineering Geology*, vol. 277, Article ID 105812, 2020.
[31] J. Wu, G. Han, M. Feng et al., "Mass-loss effects on the flow behavior in broken argillaceous red sandstone with different particle-size distributions," *Comptes Rendus Mécanique*, vol. 347, no. 6, pp. 504–523, 2019.